

**Structure, magnetization, and resistivity of  $\text{La}_{1-x}\text{M}_x\text{CoO}_3$  ( $M = \text{Ca}$ ,  $\text{Sr}$ , and  $\text{Ba}$ )**

M. Kriener, C. Zobel, A. Reichl, J. Baier, M. Cwik, K. Berggold, H. Kierspel, O. Zabara, A. Freimuth, and T. Lorenz  
*II. Physikalisches Institut, Universität zu Köln, Zùlpicher Strasse 77, 50937 Köln, Germany*

(Received 21 August 2003; revised manuscript received 17 November 2003; published 18 March 2004)

We present an investigation of the influence of structural distortions in charge-carrier doped  $\text{La}_{1-x}\text{M}_x\text{CoO}_3$  by substituting  $\text{La}^{3+}$  with alkaline-earth metals of strongly different ionic sizes, that is,  $M = \text{Ca}^{2+}$ ,  $\text{Sr}^{2+}$ , and  $\text{Ba}^{2+}$ , respectively. We find that both the magnetic properties and the resistivity change nonmonotonically as a function of the ionic size of  $M$ . Doping  $\text{La}_{1-x}\text{M}_x\text{CoO}_3$  with  $M = \text{Sr}^{2+}$  yields higher transition temperatures to the ferromagnetically ordered states and lower resistivities than doping with either  $\text{Ca}^{2+}$  or  $\text{Ba}^{2+}$  having a smaller or larger ionic size than  $\text{Sr}^{2+}$ , respectively. From this observation we conclude that the different transition temperatures and resistivities of  $\text{La}_{1-x}\text{M}_x\text{CoO}_3$  for different  $M$  (of the same concentration  $x$ ) do not only depend on the varying chemical pressures. The local disorder due to the different ionic sizes of  $\text{La}^{3+}$  and  $M^{2+}$  plays an important role, too.

DOI: 10.1103/PhysRevB.69.094417

PACS number(s): 75.30.Kz, 72.80.Ga, 71.30.+h, 71.27.+a

**I. INTRODUCTION**

Among transition-metal oxides with perovskite structure  $\text{ABO}_3$  the compound  $\text{LaCoO}_3$  is of particular interest because it shows a spin-state transition as a function of temperature. In its ground state  $\text{LaCoO}_3$  is a nonmagnetic insulator, but with increasing temperature a paramagnetic insulating state continuously develops above about 50 K and around 500 K an insulator-to-metal transition is observed. The spin-state transition may be attributed to the fact that  $\text{Co}^{3+}$  with  $3d^6$  configuration can occur in different spin states depending on the ratio of Hund's rule coupling and crystal-field splitting. The ground state of  $\text{LaCoO}_3$  is usually attributed to the low-spin configuration of  $\text{Co}^{3+}$  (LS:  $t_{2g}^6 e_g^0$ ;  $S=0$ ). However, the question whether the paramagnetic behavior above 100 K arises from a thermal population of the high-spin state (HS:  $t_{2g}^4 e_g^2$ ;  $S=2$ ) or of the intermediate-spin state (IS:  $t_{2g}^5 e_g^1$ ;  $S=1$ ) is subject of controversial discussions. Earlier publications<sup>1-5</sup> often assume a population of the HS state whereas more recent investigations<sup>6-12</sup> often favor a LS/IS scenario.

Another aspect of cobaltates that is controversially discussed in literature is the influence of charge carrier doping which can be obtained by partial substitution of three-valent  $\text{La}^{3+}$  by divalent alkaline-earth metals such as  $\text{Ca}^{2+}$ ,  $\text{Sr}^{2+}$ , or  $\text{Ba}^{2+}$ . Most studies concern the  $\text{La}_{1-x}\text{Sr}_x\text{CoO}_3$  series, where it is found that the nonmagnetic ground state is rapidly suppressed with increasing  $x$ . For small  $x$  a spin-glass behavior is observed at low temperatures whereas larger doping leads to a ferromagnetic order.<sup>3,13</sup> The resistivity strongly decreases with  $x$  and above  $x \sim 0.2$  metallic behavior is observed. These qualitative features are always found in studies on  $\text{La}_{1-x}\text{Sr}_x\text{CoO}_3$ , but the detailed phase diagrams presented so far are contradictory.<sup>3,14</sup> In some samples the transition temperatures to a spin glass or a ferromagnetic state monotonically increase with increasing Sr content,<sup>3</sup> whereas other samples show anomalies around 250 K which occur almost independent of the Sr content for  $x \geq 0.1$ .<sup>15,14</sup> It has been proposed that these differences arise from different preparation techniques.<sup>16-18</sup> Moreover, it is not clarified which spin states are present and whether or not spin-state transitions

take place as a function of temperature in the Sr-doped systems.<sup>19-21</sup>

The electronic and magnetic properties of doped  $\text{LaCoO}_3$  will not depend on the charge carrier concentration alone but also on structural parameters resulting, e.g., from chemical pressure. During the last decade the interplay between charge carrier doping and chemical pressure has been intensively studied in doped manganites and a broad variety of fascinating physical phenomena has been observed (for recent reviews see, e.g., Refs. 22-24). For doped cobaltates there are only a few studies on  $\text{La}_{1-x}\text{Ba}_x\text{CoO}_3$  (Refs. 25-27) and  $\text{La}_{1-x}\text{Ca}_x\text{CoO}_3$  (Refs. 28-35). These data indicate qualitative similarities between Ca, Sr, and Ba doping with respect to the suppression of the nonmagnetic ground state and to the occurrence of some kind of magnetic order. In this paper we present a comparative study of the structural data as well as magnetization and resistivity measurements of the series  $\text{La}_{1-x}\text{Ca}_x\text{CoO}_3$ ,  $\text{La}_{1-x}\text{Ba}_x\text{CoO}_3$ , and  $\text{La}_{1-x}\text{Sr}_x\text{CoO}_3$ .

**II. PREPARATION AND STRUCTURE**

Our samples were prepared by a standard solid-state reaction using  $\text{La}_2\text{O}_3$ ,  $\text{Co}_3\text{O}_4$ , and  $\text{MCO}_3$  ( $M = \text{Ca}$ ,  $\text{Sr}$ ,  $\text{Ba}$ ) as starting materials. The materials were mixed in the prescribed ratio and calcined in a Pt crucible at 850 °C for 48 h in air. Then the material was repeatedly reground and sintered at 1200 °C for 40 h in air. For a bare polycrystal preparation the material was finally pressed to cylindrical pellets ( $\Phi \sim 13$  mm;  $h \sim 1$  mm) by 7.5 kbar and sintered at 1200 °C for 40 h in oxygen flow. For a single-crystal growth the polycrystalline material was pressed to a cylinder ( $\Phi \sim 8$  mm;  $h \sim 10$  cm) by 2 kbar and sintered once more at 1200 °C for 20 h in air. Single crystals of  $\text{La}_{1-x}\text{Sr}_x\text{CoO}_3$  with  $0 \leq x \leq 0.3$  were grown by the traveling zone method in a four-mirror image furnace (FZ-T-10000-H-VI-VP, Crystal Systems Inc.) under oxygen atmosphere of 5 bar with typical growth velocities of 3.5 mm/h. All crystals are single phase as confirmed by powder x-ray diffraction and the Sr content, determined by energy dispersive x-ray diffraction (EDX), agrees within few percent to the nominal composition. Single crystallinity was confirmed by neutron diffraction and by Laue photographs. However, all crystals are heavily twinned

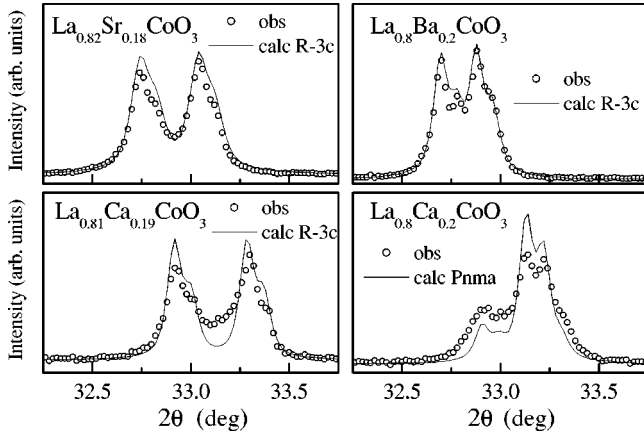


FIG. 1. Representative x-ray diffraction patterns of  $\text{La}_{1-x}\text{M}_x\text{CoO}_3$  for  $M = \text{Sr}, \text{Ba},$  and  $\text{Ca}$  with  $0.18 \leq x \leq 0.2$  around  $2\theta = 33^\circ$ . The solid lines are calculated intensities. There is a structural change of  $\text{La}_{1-x}\text{Ca}_x\text{CoO}_3$  from rhombohedral ( $R\bar{3}c$  for  $x \leq 0.19$ ) to orthorhombic symmetry ( $Pnma$  for  $x \geq 0.2$ ).

as it is usually the case for slightly distorted perovskites.

In this way we also prepared single phase polycrystals of Ba- and Ca-doped  $\text{La}_{1-x}\text{M}_x\text{CoO}_3$  with  $0 \leq x \leq 0.3$ . However, a single-crystal growth turned out to be much more difficult in these cases. From  $\text{La}_{1-x}\text{Ba}_x\text{CoO}_3$  we prepared a large single-crystal with  $x = 0.1$ , but a growth starting with  $x = 0.2$  broke down after 2 cm and the obtained rod had a Ba content of only  $x \approx 0.13$ . This problem was even more severe for  $\text{La}_{1-x}\text{Ca}_x\text{CoO}_3$ . Growth efforts starting with  $x = 0.05$  and  $0.1$  yielded crystals with Ca contents of only  $x \approx 0.03$ , whereas the EDX analysis of the remaining melts of these efforts revealed Ca contents up to  $x \approx 0.4$ . Therefore we suspect solubility limits of Ca and Ba around  $x \approx 0.03$  and  $\approx 0.13$  for our growth conditions,<sup>36</sup> whereas significantly higher doping concentration can be reached by a pure solid-state reaction. The measurements presented below were performed on polycrystals of  $\text{La}_{1-x}\text{Ba}_x\text{CoO}_3$  and  $\text{La}_{1-x}\text{Ca}_x\text{CoO}_3$  whereas in the case of  $\text{La}_{1-x}\text{Sr}_x\text{CoO}_3$  single crystals have been investigated.

The diffraction patterns of  $\text{La}_{1-x}\text{Sr}_x\text{CoO}_3$  and  $\text{La}_{1-x}\text{Ba}_x\text{CoO}_3$  can be indexed by a rhombohedral unit cell containing 2 formula units (space group  $R\bar{3}c$ ). We note that a recent high-resolution single-crystal x-ray study of the undoped  $\text{LaCoO}_3$  revealed a small monoclinic distortion, which is related to a Jahn-Teller effect of the thermally excited  $\text{Co}^{3+}$  ions in the intermediate-spin state,<sup>37</sup> but the observed distortion in  $\text{LaCoO}_3$  is too small to be observed in a usual powder x-ray analysis.  $\text{La}_{1-x}\text{Ca}_x\text{CoO}_3$  with  $x \leq 0.19$  also has rhombohedral symmetry, but for  $x \geq 0.2$  there is a structural change to orthorhombic symmetry ( $Pnma$ ), which can be best visualized around  $2\theta = 33^\circ$  in the diffraction pattern. As shown in Fig. 1 the patterns of the Sr- and Ba-doped samples and for the Ca-doped sample with  $x = 0.19$  are very similar and well described by  $R\bar{3}c$  symmetry. However, the pattern of  $\text{La}_{1-x}\text{Ca}_x\text{CoO}_3$  with  $x = 0.2$  is systematically different and a description within  $Pnma$  symmetry is clearly better than within  $R\bar{3}c$ . In this respect our result differs from those of

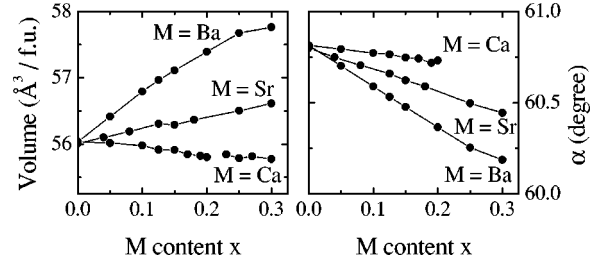


FIG. 2. Volume per formula unit (left) and rhombohedral angle  $\alpha_R$  (right) as a function of doping for  $\text{La}_{1-x}\text{M}_x\text{CoO}_3$  with  $M = \text{Ba}, \text{Sr},$  and  $\text{Ca}$ . In  $\text{La}_{1-x}\text{Ca}_x\text{CoO}_3$  symmetry changes to orthorhombic ( $Pnma$ ) for  $x \geq 0.2$ .

Refs. 28 and 29, where the rhombohedral symmetry was used also for  $x > 0.2$ , and of Ref. 33, where a two-phase region consisting of an admixture of a rhombohedral and a pseudocubic phase was proposed for  $x > 0.2$ .

In Fig. 2 we compare the doping dependencies of the volume per formula unit and of the rhombohedral angle  $\alpha_R$  for all three series. The volume increases strongly with increasing Ba and moderately with increasing Sr content whereas Ca doping causes a slight decrease of the unit volume. For all three dopings the rhombohedral angle systematically decreases with increasing content of  $M$ . For Ca doping a transition to orthorhombic symmetry takes place. For Ba and Sr doping cubic symmetry ( $\alpha_R = 60^\circ$ ) is approached and, from a linear extrapolation of our data, is expected to occur around  $x = 0.37$  and  $0.67$ , respectively. This value agrees well with the observed cubic symmetry in  $\text{La}_{1-x}\text{Ba}_x\text{CoO}_3$  for  $x = 0.4$ ,<sup>38</sup> but is too large for  $\text{La}_{1-x}\text{Sr}_x\text{CoO}_3$  where a cubic structure was reported already for  $x = 0.5$ .<sup>39</sup>

### III. MAGNETIZATION

In Fig. 3 we compare the magnetization of all three  $\text{La}_{1-x}\text{M}_x\text{CoO}_3$  series as a function of temperature. A magnetic field of 50 mT has been applied at 300 K, then the sample was cooled to 4 K and the data were taken during the subsequent heating run. The undoped  $\text{LaCoO}_3$  shows a pronounced maximum of  $M(T)$  around 90 K arising from the spin-state transition of the  $\text{Co}^{3+}$  ions [Fig. 3(a)]. In Ref. 12 we have presented a combined analysis of this  $M(T)$  curve and the thermal expansion of  $\text{LaCoO}_3$ , which gives evidence for a low-spin to intermediate-spin state scenario. A maximum of  $M(T)$  is also present for  $x = 0.002$ , but not visible anymore for  $x \geq 0.01$ . The samples with  $0.04 \leq x \leq 0.15$  show a kink or a peak in  $M(T)$  indicating a spin-glass behavior at low temperatures [Fig. 3(b)], whereas the crystals with  $x \geq 0.18$  show a continuously increasing spontaneous magnetization with decreasing temperature as expected for a usual ferromagnet [Fig. 3(c)]. At low temperatures all  $\text{La}_{1-x}\text{Sr}_x\text{CoO}_3$  crystals show differences between the  $M(T)$  curves obtained in the field-cooled (FC) run and the corresponding curves obtained in a zero-field-cooled (ZFC) run (not shown), when the magnetic field is applied at the lowest temperature after the sample has been cooled in zero field. Such a difference is expected for a spin glass, but this differ-

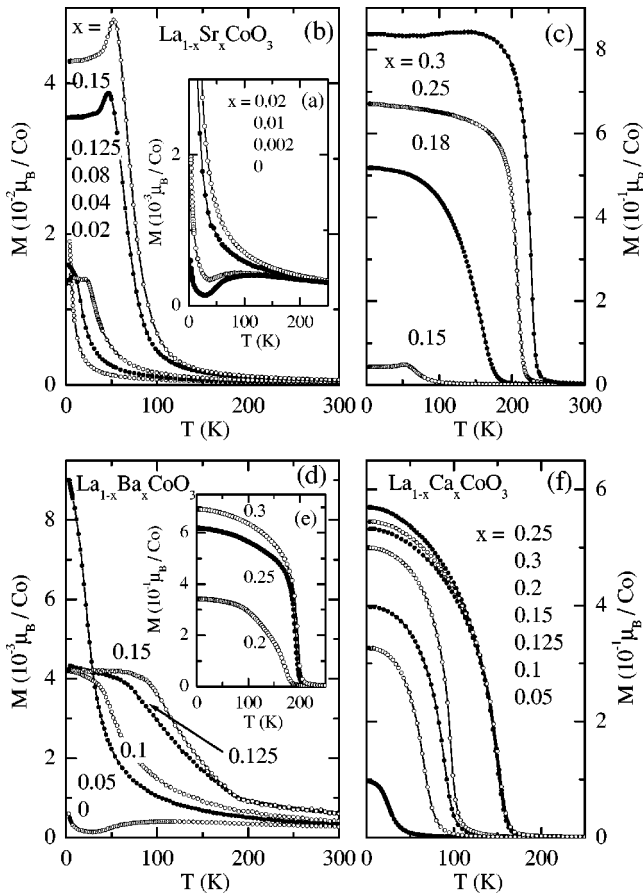


FIG. 3. Magnetization vs temperature of  $\text{La}_{1-x}\text{Sr}_x\text{CoO}_3$  (a–c),  $\text{La}_{1-x}\text{Ba}_x\text{CoO}_3$  (d, e), and  $\text{La}_{1-x}\text{Ca}_x\text{CoO}_3$  (f). All curves were taken during field-cooled runs in an applied magnetic field of 50 mT. Please note the different orders of magnitude of  $M$  for the different panels.

ence alone does not prove spin-glass behavior, since it can also arise from the domain structure of a ferromagnet. In order to distinguish between spin-glass freezing or ferromagnetic order, one has to perform time-dependent studies, such as ac-susceptibility measurements of different frequencies or relaxation studies of the magnetization. From such studies it has been concluded that  $\text{La}_{1-x}\text{Sr}_x\text{CoO}_3$  shows a spin-glass behavior for  $x < 0.18$  and the occurrence of a so-called cluster spin glass has been proposed for  $0.18 \leq x \leq 0.5$ .<sup>3</sup> Our results of  $M(T)$  agree with such an interpretation, but for the reasons explained above we cannot confirm with ambiguity this conclusion. For the sake of simplicity we will not try to discriminate between a cluster spin glass and a ferromagnet in the following.

The magnetization of the Ba-doped samples with  $x = 0.05$  and  $0.1$  continuously increases with decreasing temperature and below a certain temperature the curves flatten as is clearly seen for the  $x = 0.1$  sample [Fig. 3(d)]. Although more difficult to see, the flattening is also present for  $x = 0.05$  as we have identified from a plot of  $1/M$  vs  $T$  (not shown). Insofar the Ba-doped samples with  $x = 0.05$  and  $x = 0.1$  show a very similar behavior to the Sr-doped ones with  $x = 0.04$  and  $0.08$ . With increasing Ba doping the flattening

of  $M(T)$  becomes more pronounced and another clear kink in  $M(T)$  occurs around 200 K. It is remarkable that all Ba-doped samples with  $0.1 \leq x \leq 0.15$  show almost the same low-temperature value of  $M$ . This is in contrast to the corresponding Sr-doped samples, where  $M$  at the lowest temperatures continuously increases with  $x$ . In addition, the Ba-doped samples do not show a peak in the FC  $M(T)$  curves. For higher Ba concentrations ( $x \geq 0.2$ ) a pronounced spontaneous magnetization occurs as in a conventional ferromagnet and both the absolute value of  $M$  and the transition temperature  $T_c$  systematically increase with  $x$  [Fig. 3(e)].

The  $M(T)$  curves of  $\text{La}_{1-x}\text{Ca}_x\text{CoO}_3$  [Fig. 3(f)] differ from those of the Ba- and Sr-doped series because the principal temperature dependence does hardly change as a function of Ca content. Already the sample with  $x = 0.05$  shows a spontaneous magnetization with a temperature dependence typical for a ferromagnet and the absolute value of  $M(4\text{ K})$  is about one order of magnitude larger than those of the corresponding Sr- and Ba-doped samples. With increasing Ca concentration both  $T_c$  and the absolute value of  $M(4\text{ K})$  systematically increase with  $x$  up to  $x = 0.2$  and remain essentially constant for  $0.2 \leq x \leq 0.3$ . The different  $M(4\text{ K})$  values which depend nonmonotonically on  $x$  cannot be taken seriously, since for technical reasons we had to use extremely small samples. Therefore the error in weighing the samples is of order 10%, which is larger than the differences in  $M(4\text{ K})$ .

Figure 4 gives an overview of the magnetization curves measured at 4 K for all three series.  $\text{La}_{1-x}\text{Ca}_x\text{CoO}_3$  shows the typical behavior of a ferromagnet with a large hysteresis region. With increasing  $x$  the hysteresis narrows and the absolute value of the magnetization increases slightly. For both samples the magnetization strongly flattens in the higher-field range but the saturation is apparently not yet reached. For the  $\text{La}_{1-x}\text{Sr}_x\text{CoO}_3$  series the form of the magnetization curves changes as a function of  $x$ . The  $x = 0.25$  sample has only a very small hysteresis (see inset of Fig. 4) and the magnetization is essentially saturated in a field of 6 T. For  $x = 0.18$  the magnetization becomes smaller and the hysteresis larger, but the  $M(B)$  curve still has the form of a typical ferromagnet. The form of  $M(B)$  changes when the Sr content is reduced to  $x = 0.125$ . The hysteresis region becomes very broad and there is no steep change of  $M$  around the coercive field. This difference can be interpreted as further indication of a transition from spin-glass behavior to a ferromagnet (or a cluster spin glass) around  $x \approx 0.18$ . A very broad hysteresis is also present in  $\text{La}_{1-x}\text{Ba}_x\text{CoO}_3$ . As shown in the lower inset of Fig. 4 the Ba-doped sample with  $x = 0.1$  has a small hysteresis that extends even up to the maximum field of 6 T. Similar  $M(B)$  curves are found in the entire range  $0.05 \leq x \leq 0.15$  of Ba doping. The samples with  $x \geq 0.2$  have again more conventional  $M(B)$  curves with hysteresis widths which are somewhat smaller and larger than those of the corresponding Ca- and Sr-doped samples, respectively. However, a closer inspection of Fig. 4 reveals another anomaly:  $\text{La}_{0.75}\text{Ba}_{0.25}\text{CoO}_3$  has a virgin curve of  $M(B)$  that is located *outside* of the subsequent hysteresis loop over a large field range. This anomalous behavior is

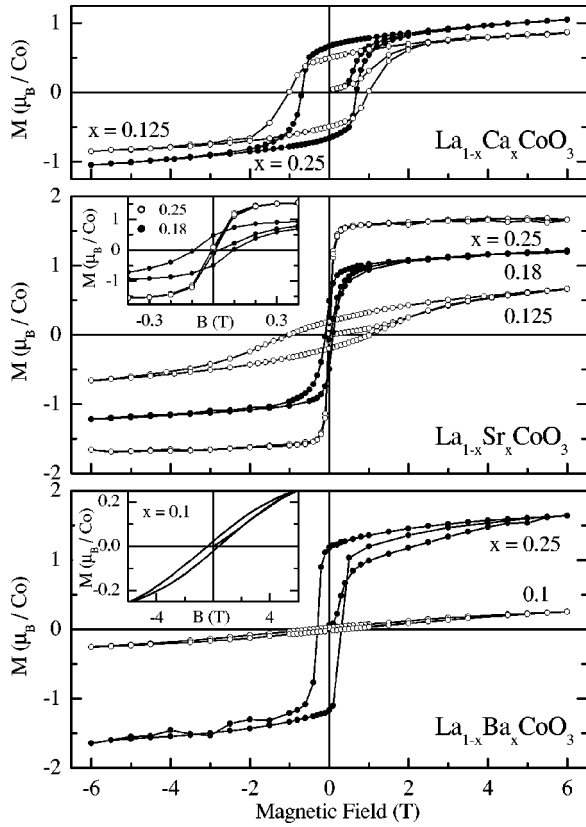


FIG. 4. Magnetization curves of  $\text{La}_{1-x}\text{Ca}_x\text{CoO}_3$  (top),  $\text{La}_{1-x}\text{Sr}_x\text{CoO}_3$  (middle), and  $\text{La}_{1-x}\text{Ba}_x\text{CoO}_3$  (bottom) measured at  $T=4$  K. The inset of the middle panel is an expanded view of the low-field region for the Sr-doped samples with  $x=0.18$  and  $0.25$  showing that the hysteresis of the latter sample is extremely small. The inset of the bottom panel is an expanded view of  $M(B)$  of  $\text{La}_{0.9}\text{Ba}_{0.1}\text{CoO}_3$  which has a small hysteresis over the entire field range.

well reproducible and occurs also for  $x=0.3$ . To the best of our knowledge these anomalous virgin curves are neither expected for a ferromagnet nor for a spin glass.

#### IV. RESISTIVITY

Figure 5 compares the resistivity data of the  $\text{La}_{1-x}\text{M}_x\text{CoO}_3$  series. In agreement with previous studies the undoped  $\text{LaCoO}_3$  is a good insulator at low temperatures and shows an insulator-to-metal transition around 500 K. Below 400 K  $\rho$  shows an activation type behavior  $\rho \propto \exp(\Delta_{act}/T)$  down to 50 K with activation energy  $\Delta_{act} \approx 1240$  K. The weakly doped samples ( $x \leq 0.04$ ) show qualitatively similar resistivity behavior as the pure compound, but the  $\log(\rho)$  vs  $1/T$  curves are not linear [Fig. 5(b)]. With further increasing Sr content the low-temperature  $\rho$  rapidly drops and the samples above  $x=0.18$  show a metallic temperature dependence of  $\rho$  over the entire temperature range [Fig. 5(a)]. The crystals with  $x=0.18$ ,  $0.25$ , and  $0.3$  show distinct anomalies in  $\rho(T)$  at the critical temperatures of ferromagnetic order [Fig. 5(c)].

A drastic decrease of  $\rho$  with increasing concentration is also found for Ca and Ba doping, but there are no Ca- or

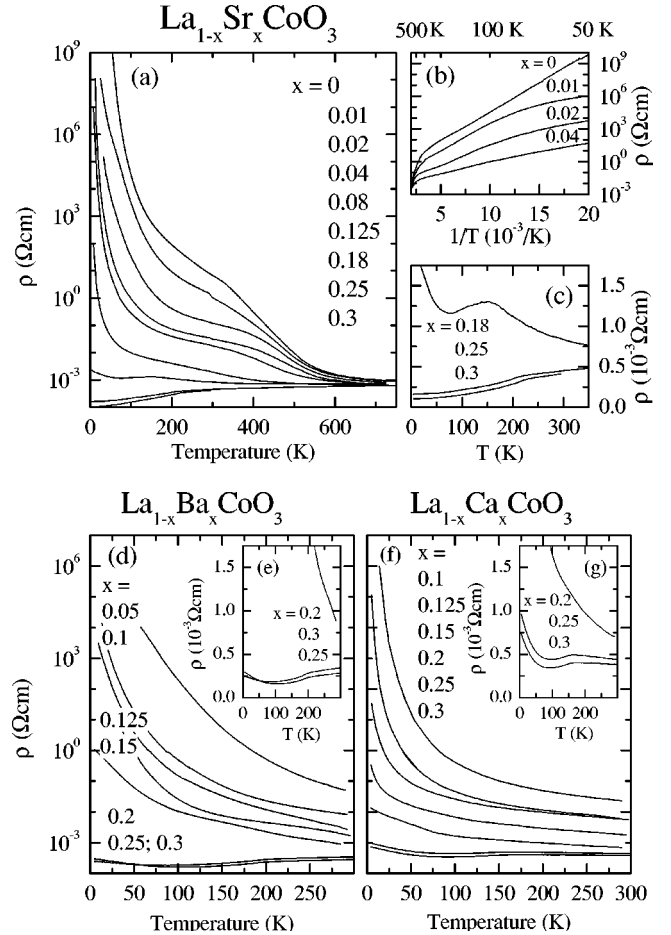


FIG. 5. Resistivity vs temperature of  $\text{La}_{1-x}\text{Sr}_x\text{CoO}_3$  (a–c),  $\text{La}_{1-x}\text{Ba}_x\text{CoO}_3$  (d, e), and  $\text{La}_{1-x}\text{Ca}_x\text{CoO}_3$  (f, g). Panel (b) shows Arrhenius plots  $\log(\rho)$  vs  $1/T$  for the low-Sr-doped samples ( $x \leq 0.04$ ) and panels (c), (e), and (f) give expanded views of the low-temperature resistivities on a linear scale of the (nearly) metallic samples ( $x \geq 0.18$ ).

Ba-doped samples showing metallic resistivity behavior over the entire temperature range. From the Ba-doped series only the samples with  $x \geq 0.25$  have a decreasing  $\rho$  with decreasing temperature from 300 K down to about 100 K with clear slope changes around 200 K [Fig. 5(e)], where ferromagnetic order sets in. Insofar the  $\rho(T)$  curves of the higher Ba-doped samples are similar to those of higher Sr-doped crystals, but with further decreasing temperature the resistivities of the Ba-doped samples increase again. From the Ca-doped series even the samples with  $x=0.25$  and  $0.3$  show a weakly increasing  $\rho$  with decreasing temperature from 300 K down to about 150 K [Fig. 5(g)]. Then there is a slight decrease of  $\rho(T)$  below about 150 K, which is again the ferromagnetic ordering temperature. Finally, both Ca-doped samples show a low-temperature increase of  $\rho$  below about 80 K that is even more pronounced than in the Ba-doped samples. One might suspect that the low-temperature increase of  $\rho$  arises from the fact that the Ca- and Ba-doped samples are polycrystals whereas the Sr-doped ones are single crystals. However, this is not the only reason for the different low-temperature behavior. We have measured  $\rho$  of polycrystalline

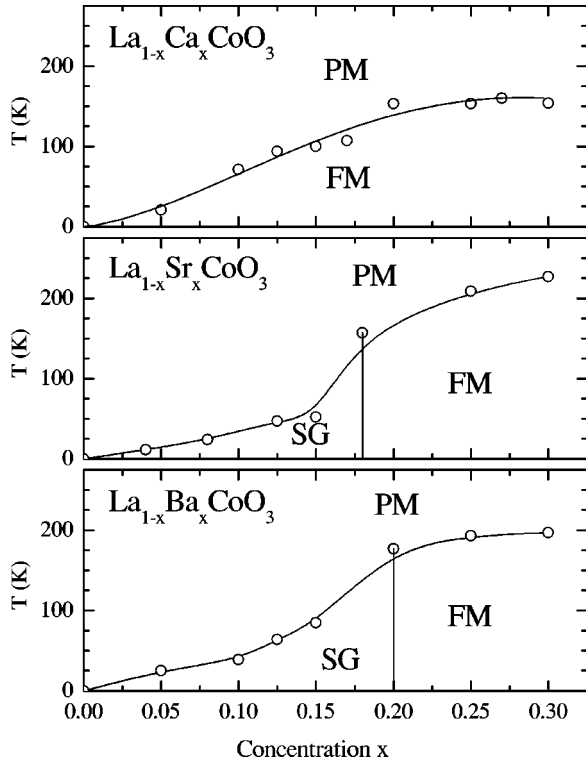


FIG. 6. Phase diagrams of  $\text{La}_{1-x}\text{M}_x\text{CoO}_3$  with  $M = \text{Ba}, \text{Sr},$  and  $\text{Ca}$  (from bottom to top). PM, FM, and SG stand for paramagnet, ferromagnet, and spin glass, respectively. The solid lines are to guide the eye. We mention, however, that an unambiguous distinction between a SG and a FM (or the so-called cluster glass phase proposed in Ref. 3 for  $\text{La}_{1-x}\text{Sr}_x\text{CoO}_3$  with  $x > 0.18$ ) is not possible from our measurements of the static magnetization alone.

$\text{La}_{0.7}\text{Sr}_{0.3}\text{CoO}_3$  and found that it also shows a low-temperature increase, but this increase is weaker than in the Ba-doped and much weaker than in the Ca-doped polycrystal.

## V. DISCUSSION

In Fig. 6 we summarize the phase diagrams obtained from the magnetization measurements. For  $\text{La}_{1-x}\text{Ca}_x\text{CoO}_3$  we find transitions from a paramagnetic to a ferromagnetic phase for the entire concentration range. The transition temperature  $T_c$  monotonously increases with  $x$  for  $x \leq 0.2$  and tends to saturate around  $T_c \sim 150$  K for larger  $x$ . Our results of the Sr-doped series nicely agree with those obtained by Itoh *et al.*<sup>3</sup> For  $x \leq 0.18$  the magnetization has features which are typical for the proposed spin-glass behavior and the characteristic temperature  $T_c$  strongly increases when  $x = 0.18$  is approached. For larger  $x$  the  $M(T)$  curves resemble those of typical ferromagnets and  $T_c$  increases up to about 230 K for  $x = 0.3$ . We emphasize that additional anomalous features in the  $M(T)$  curves around 240 K, which have been frequently observed in polycrystalline  $\text{La}_{1-x}\text{Sr}_x\text{CoO}_3$  for a large doping range  $0.025 \leq x \leq 0.5$ ,<sup>14,15</sup> do not occur in our single crystals. Thus, we conclude that these features are not intrinsic properties of  $\text{La}_{1-x}\text{Sr}_x\text{CoO}_3$  but rather arise from the different preparation technique of those polycrystals as has been pro-

posed in Refs. 16–18. The Ba-doped series has qualitatively similar  $M(T)$  curves as the Sr-doped samples. Thus, we conclude that  $\text{La}_{1-x}\text{Ba}_x\text{CoO}_3$  shows a spin-glass behavior for  $x < 0.2$  and a ferromagnetic order for larger  $x$  with a saturation of  $T_c$  around 200 K.

For  $x \geq 0.2$  all three series of  $\text{La}_{1-x}\text{M}_x\text{CoO}_3$  show ferromagnetic order and for a given  $x$  the Sr-doped samples have the largest  $T_c$  values ( $\sim 220$  K), the Ba-doped samples have somewhat smaller ( $\sim 200$  K) and the Ca-doped samples significantly smaller  $T_c$ 's ( $\sim 150$  K). Obviously,  $T_c$  depends nonmonotonically on the ionic size of  $M$ . Since the less conducting  $\text{La}_{1-x}\text{Ca}_x\text{CoO}_3$  samples have the lowest transition temperatures one may suspect a correlation between metallic conductivity and ferromagnetic order as it would be expected within a double-exchange model. However, the Ba-doped samples have lower  $T_c$  values than the Sr-doped ones although their resistivities are comparable or even slightly smaller than those of the Sr-doped samples.

In doped manganites  $\text{La}_{1-x}\text{M}_x\text{MnO}_3$   $T_c$  also depends nonmonotonically on the ionic sizes of  $M = \text{Ca}, \text{Sr},$  and  $\text{Ba}$  for  $x \geq 0.15$ .<sup>40–42</sup> In the manganite case it is argued that the transition temperature is mainly determined by two kinds of structural distortions.<sup>43</sup> The first is a global distortion arising from the deviation of the structure from the cubic perovskite. This distortion can be described by the deviation of the tolerance factor  $t = (\langle r_A \rangle + r_O) / [\sqrt{2}(r_{Mn} + r_O)]$  from  $t = 1$  where  $r_{Mn}$  and  $r_O$  denote the ionic radii of the Mn and O ions and  $\langle r_A \rangle = (1-x)r_{La} + xr_M$  is the average radius of the ions on the A site, that is, the average of the radii of  $\text{La}^{3+}$  and  $M^{2+} = \text{Ca}^{2+}, \text{Sr}^{2+},$  or  $\text{Ba}^{2+}$ , respectively. The second type is a local distortion arising from the different ionic radii of  $\text{La}^{3+}$  and  $M^{2+}$ , which can be described by the variance of the A-site ionic radii  $\sigma^2 = (1-x)r_{La}^2 + xr_M^2 - \langle r_A \rangle^2$ . In order to quantify these two phenomena the following empirical relation was proposed:<sup>43</sup>

$$T_c(\langle r_A \rangle, \sigma) = T_c(r_A^0, 0) - p_1 Q_0^2 - p_2 \sigma^2. \quad (1)$$

Here,  $T_c(\langle r_A \rangle, \sigma)$  is the real transition temperature and  $T_c(r_A^0, 0)$  is a hypothetical transition temperature of an ideal cubic perovskite with A-site ion radius  $r_A^0$  that fulfills  $t = 1$  and  $\sigma = 0$ . The deviation from cubic symmetry is given by  $Q_0 = r_A^0 - \langle r_A \rangle$  and  $p_1$  and  $p_2$  are constants. We use the tabulated ionic radii 1.35 Å for  $\text{O}^{2-}$  and 1.216 Å, 1.18 Å, 1.31 Å, and 1.47 Å for the A-site ions  $\text{La}^{3+}, \text{Ca}^{2+}, \text{Sr}^{2+},$  and  $\text{Ba}^{2+}$  in nine-fold coordination<sup>44,45</sup> and for  $r_A^0 = 0.6r_{La} + 0.4r_{Ba} \approx 1.32$  Å since  $\text{La}_{1-x}\text{Ba}_x\text{CoO}_3$  becomes cubic for  $x = 0.4$ .<sup>25</sup> These values yield for the remaining parameters  $p_1 \approx 6.1 \times 10^3 \text{ K}/\text{Å}^2$ ,  $p_2 \approx 3.4 \times 10^3 \text{ K}/\text{Å}^2$ , and  $T_c(r_A^0, 0) \approx 229$  K for  $x = 0.2$ .<sup>46</sup> The corresponding values for  $x = 0.25$  are  $10.3 \times 10^3 \text{ K}/\text{Å}^2$ ,  $6.3 \times 10^3 \text{ K}/\text{Å}^2$ , and 286 K and those for  $x = 0.3$  are  $11.4 \times 10^3 \text{ K}/\text{Å}^2$ ,  $7.4 \times 10^3 \text{ K}/\text{Å}^2$ , and 306 K.

For all three series the observed  $T_c$  values are significantly reduced from those of the corresponding hypothetical, ideal cubic perovskites. For  $\text{La}_{1-x}\text{Ca}_x\text{CoO}_3$  the reduction is most pronounced although in this case the effect of the A-site disorder is negligibly small ( $\sigma^2$  is of order  $10^{-4} \text{ Å}^2$ ) be-

cause the ionic radii of  $\text{La}^{3+}$  and  $\text{Ca}^{2+}$  are very close to each other. The reduction is almost completely a consequence of the deviation from cubic symmetry which is most pronounced in  $\text{La}_{1-x}\text{Ca}_x\text{CoO}_3$ . This global distortion is already rather large in the undoped  $\text{LaCoO}_3$  and increases with increasing substitution of La by the smaller Ca ion. This is consistent with our observation of a structural phase transition from rhombohedral to orthorhombic which is expected for perovskites when the tolerance factor becomes smaller. For Sr doping the A-site disorder is larger ( $\sigma^2$  is of order  $10^{-3} \text{ \AA}^2$ ) than for Ca doping, but the  $T_c$  reduction due to this effect remains small (of order 10 K). The Sr-doped samples have significantly larger  $T_c$  values than the Ca-doped ones, since the structure approaches cubic symmetry and therefore the reduction of  $T_c$  due to the global distortion is less pronounced. For Ba doping the structure further approaches cubic symmetry and consequently the influence of the global distortion on  $T_c$  is further reduced. However, the A-site disorder is now pretty large ( $\sigma^2$  is of order  $10^{-2} \text{ \AA}^2$ ), since  $\text{Ba}^{2+}$  is much larger than  $\text{La}^{3+}$ . In the case of Ba doping the  $T_c$  reduction due to the deviation from cubic symmetry is only of order 15 K, but the reduction due to A-site disorder increases from about 30 K to 95 K when  $x$  increases from 0.2 to 0.3 and explains why the  $T_c$  values of  $\text{La}_{1-x}\text{Ba}_x\text{CoO}_3$  do not exceed those of  $\text{La}_{1-x}\text{Sr}_x\text{CoO}_3$ .

Considering the global and local distortions in  $\text{La}_{1-x}\text{M}_x\text{CoO}_3$  also allows to give some qualitative arguments for the different resistivity behavior for different M. Since for the Ca-doped samples the deviation from cubic symmetry is most pronounced, there is a rather strong deviation of the Co-O-Co bond angle from  $180^\circ$  and the hopping integral, or in other words the bandwidth, is small. As a consequence the  $\rho(T)$  curves of  $\text{La}_{1-x}\text{Ca}_x\text{CoO}_3$  remain almost semiconducting even for  $x=0.3$ . In  $\text{La}_{1-x}\text{Sr}_x\text{CoO}_3$  the Co-O-Co angle is closer to  $180^\circ$  and consequently the bandwidth increases leading to metallic  $\rho(T)$  curves for  $x > 0.18$ . In  $\text{La}_{1-x}\text{Ba}_x\text{CoO}_3$  the bandwidth will be even larger than in the Sr-doped samples in agreement with the smaller resistivities we observe at temperatures above about 100 K. Yet, the  $\rho(T)$  curves for Ba doping with  $x \geq 0.25$  show a low-temperature increase. This may arise from a larger local disorder in  $\text{La}_{1-x}\text{Ba}_x\text{CoO}_3$  making these samples more sensitive to charge localization at low temperatures than the Sr-doped samples.

Next we will discuss the doping range below  $x=0.2$ , where the Sr- and Ba-doped series show spin-glass behavior which is absent in  $\text{La}_{1-x}\text{Ca}_x\text{CoO}_3$ . One source for spin-glass behavior are competing ferromagnetic and antiferromagnetic interactions. Such a competition may arise from local disorder which will be more pronounced in the Sr- and Ba-doped samples due to the larger A-site disorder than for Ca doping. Thus, the absence of spin-glass behavior in  $\text{La}_{1-x}\text{Ca}_x\text{CoO}_3$  may arise from the similar ionic radii of  $\text{La}^{3+}$  and  $\text{Ca}^{2+}$ . Another reason could arise from the structural phase transition of  $\text{La}_{1-x}\text{Ca}_x\text{CoO}_3$ . This transition is located at room temperature for  $x=0.2$  and possibly shifts towards lower temperatures for smaller  $x$ . If one assumes that the ferromagnetic exchange is enhanced in the orthorhombic structure, a

further reason for the ferromagnetic order in low-doped  $\text{La}_{1-x}\text{Ca}_x\text{CoO}_3$  could be that these samples are orthorhombic at low temperatures.

As mentioned in the Introduction it is not clear which spin states of the  $\text{Co}^{3+}$  and  $\text{Co}^{4+}$  ions are realized in  $\text{La}_{1-x}\text{M}_x\text{CoO}_3$  samples, and it is not known whether there are spin-state transitions as a function of temperature. From our present data we cannot unambiguously resolve these puzzles. Clear indications of spin-state transitions are only present in the  $M(T)$  curves of the  $\text{La}_{1-x}\text{Sr}_x\text{CoO}_3$  samples with very low doping ( $x < 0.01$ ). For larger dopings the  $M(T)$  curves are dominated by the occurrence of spin-glass or ferromagnetically ordered phases. The saturation values of the magnetization in the ferromagnetic phases with  $x=0.25$  amount to  $M_S \sim 1 \mu_B/\text{Co}$  for Ca- and to  $\sim 1.65 \mu_B/\text{Co}$  for Sr and Ba doping. The latter value fits best to the expected spin-only value of  $\sim 1.75 \mu_B/\text{Co}$  expected for a  $\text{Co}^{4+}$  LS state ( $t_{2g}^5 e_g^0$ ) and a  $\text{Co}^{3+}$  IS state ( $t_{2g}^5 e_g^1$ ). If these spin states are realized one can easily imagine the relevance of the double exchange mechanism and understand the similarity to the manganites, because these spin states differ only by two additional down-spin electrons in the  $t_{2g}$  level from the corresponding high-spin states of  $\text{Mn}^{4+}$  ( $t_{2g}^3 e_g^0$ ) and  $\text{Mn}^{3+}$  ( $t_{2g}^3 e_g^1$ ). In view of the much lower value of  $M_S$  observed in the Ca-doped sample this very simplified picture of considering spin-only values remains, however, questionable.

## VI. SUMMARY

We have presented a comparative study of the structure, magnetization, and resistivity of charge-carrier doped  $\text{La}_{1-x}\text{M}_x\text{CoO}_3$  with  $M = \text{Ca}, \text{Sr}, \text{and Ba}$  ( $0 \leq x \leq 0.3$ ). The Sr- and Ba-doped samples crystallize in a rhombohedral structure, which slowly (moderately fast) approaches cubic symmetry with increasing Sr (Ba) content. For  $\text{La}_{1-x}\text{Ca}_x\text{CoO}_3$  there is a structural phase transition from rhombohedral to orthorhombic symmetry for  $x \geq 0.2$ . For all three series the resistivity rapidly decreases with increasing concentration of M. For Ca doping the  $\rho(T)$  curves do not reach a metallic temperature dependence, whereas the Sr-doped crystals become metallic for  $x > 0.18$ . The Ba-doped samples are metallic above about 100 K for  $x \geq 0.25$ , but there are pronounced localization effects for low temperatures. The different resistivities may be explained by an increasing bandwidth with increasing ionic radii of the  $M^{2+}$  ions on the one hand side and by local disorder due to the different ionic radii of  $\text{La}^{3+}$  and  $M^{2+}$  on the other. The  $M(T)$  curves indicate spin-glass behavior at low temperatures for the Ba- and Sr-doped samples with  $x < 0.2$  and  $0.18$ , respectively, whereas for larger  $x$  ferromagnetic order occurs. In contrast, the  $\text{La}_{1-x}\text{Ca}_x\text{CoO}_3$  samples show ferromagnetic order over the entire doping range. The reason for the absence of the spin glass region in  $\text{La}_{1-x}\text{Ca}_x\text{CoO}_3$  remains to be clarified. The ferromagnetic order occurs at the largest ordering temperatures  $T_c(x)$  for Sr doping, for Ba doping  $T_c(x)$  is slightly smaller, and for Ca doping significantly smaller. Similar to the case of doped manganites<sup>45</sup> this non-monotonic dependence of  $T_c$  on the ionic radii of  $M^{2+}$  can

be phenomenologically explained by assuming that the largest  $T_c(x)$  would be obtained in a perfectly cubic perovskite without disorder and is reduced by both a deviation from cubic symmetry and local disorder due to different radii of  $\text{La}^{3+}$  and  $M^{2+}$ .  $\text{La}_{1-x}\text{Sr}_x\text{CoO}_3$  has higher  $T_c$  values, since  $T_c$  is strongly suppressed by a large deviation from cubic symmetry in  $\text{La}_{1-x}\text{Ca}_x\text{CoO}_3$  and by pronounced local disorder in  $\text{La}_{1-x}\text{Ba}_x\text{CoO}_3$ .

## ACKNOWLEDGMENTS

We acknowledge fruitful discussions with M. Braden, J. B. Goodenough, M. Grüninger, D. Khomskii, and L. H. Tjeng. We thank G. Dhalenne, P. Reutler, and A. Revcolevschi for their help when we were growing our first single crystals. This work was supported by the Deutsche Forschungsgemeinschaft through SFB 608.

- <sup>1</sup>P.M. Raccach and J.B. Goodenough, *Phys. Rev.* **155**, 932 (1967).
- <sup>2</sup>K. Asai, O. Yokokura, N. Nishimori, H. Chou, J.M. Tranquada, G. Shirane, S. Higuchi, Y. Okajima, and K. Kohn, *Phys. Rev. B* **50**, 3025 (1994).
- <sup>3</sup>M. Itoh, I. Natori, S. Kubota, and K. Motoya, *J. Phys. Soc. Jpn.* **63**, 1486 (1994).
- <sup>4</sup>M.A. Senarís-Rodríguez and J.B. Goodenough, *J. Solid State Chem.* **116**, 224 (1995).
- <sup>5</sup>S. Yamaguchi, Y. Okimoto, H. Taniguchi, and Y. Tokura, *Phys. Rev. B* **53**, 2926 (1996).
- <sup>6</sup>R.H. Potze, G.A. Sawatzky, and M. Abbate, *Phys. Rev. B* **51**, 11 501 (1995).
- <sup>7</sup>M.A. Korotin, S.Y. Ezhov, I.V. Solovyev, V.I. Anisimov, D.I. Khomskii, and G.A. Sawatzky, *Phys. Rev. B* **54**, 5309 (1996).
- <sup>8</sup>T. Saitoh, T. Mizokawa, A. Fujimori, M. Abbate, Y. Takeda, and M. Takano, *Phys. Rev. B* **55**, 4257 (1997).
- <sup>9</sup>K. Asai, A. Yoneda, O. Yokokura, J.M. Tranquada, G. Shirane, and K. Kohn, *J. Phys. Soc. Jpn.* **67**, 290 (1998).
- <sup>10</sup>S. Yamaguchi, Y. Okimoto, and Y. Tokura, *Phys. Rev. B* **55**, 8666 (1997).
- <sup>11</sup>Y. Kobayashi, N. Fujiwara, S. Murata, K. Asai, and H. Yasuoka, *Phys. Rev. B* **62**, 410 (2000).
- <sup>12</sup>C. Zobel, M. Kriener, D. Bruns, J. Baier, M. Grüninger, T. Lorenz, P. Reutler, and A. Revcolevschi, *Phys. Rev. B* **66**, 020402 (2002).
- <sup>13</sup>V.G. Sathe, A.V. Pimpale, V. Siruguri, and S.K. Paranjpe, *J. Phys.: Condens. Matter* **8**, 3889 (1996).
- <sup>14</sup>M.A. Senarís-Rodríguez and J.B. Goodenough, *J. Solid State Chem.* **118**, 323 (1995).
- <sup>15</sup>R. Caciuffo, D. Rinaldi, G. Barucca, J. Mira, J. Rivas, M.A. Senarís-Rodríguez, P.G. Radaelli, D. Fiorani, and J.B. Goodenough, *Phys. Rev. B* **59**, 1068 (1999).
- <sup>16</sup>V. Golovanov, L. Mihaly, and A.R. Moodenbaugh, *Phys. Rev. B* **53**, 8207 (1996).
- <sup>17</sup>P.S. Anil Kumar, P.A. Joy, and S.K. Date, *J. Appl. Phys.* **83**, 7375 (1998).
- <sup>18</sup>P.A. Joy and S.K. Date, *J. Phys.: Condens. Matter* **11**, L217 (1999).
- <sup>19</sup>F. Munakata, H. Takahashi, Y. Akimune, Y. Shichi, M. Tanimura, Y. Inoue, R. Itti, and Y. Koyama, *Phys. Rev. B* **56**, 979 (1997).
- <sup>20</sup>A. Chainani, M. Mathew, and D.D. Sarma, *Phys. Rev. B* **46**, 9976 (1992).
- <sup>21</sup>K. Tsutsui, J. Inoue, and S. Maekawa, *Phys. Rev. B* **59**, 4549 (1999).
- <sup>22</sup>M.B. Salamon and M. Jaime, *Rev. Mod. Phys.* **73**, 583 (2001).
- <sup>23</sup>C.N.R. Rao, A. Arulraj, A.K. Cheetham, and B. Raveau, *J. Phys.: Condens. Matter* **12**, R83 (2000).
- <sup>24</sup>J.M.D. Coey, M. Viret, and S. von Molnar, *Adv. Phys.* **48**, 167 (1999).
- <sup>25</sup>S.B. Patil, H.V. Keer, and D.K. Chakrabarty, *Phys. Status Solidi A* **52**, 681 (1979).
- <sup>26</sup>F. Fauth, E. Suard, and V. Caignaert, *Phys. Rev. B* **65**, 060401 (2001).
- <sup>27</sup>J. Wang, Z.D. Wang, W. Zhang, and D.Y. Xing, *Phys. Rev. B* **66**, 064406 (2002).
- <sup>28</sup>H. Taguchi, M. Shimada, and M. Koizumi, *J. Solid State Chem.* **41**, 329 (1982).
- <sup>29</sup>Ch. Zock, L. Haupt, K. Bärner, B.M. Todris, K. Asadov, E.A. Zavadskii, and T. Gron, *J. Magn. Magn. Mater.* **150**, 253 (1995).
- <sup>30</sup>N.-C. Yeh, R.P. Vasquez, D.A. Beam, C.-C. Fu, J. Huynh, and G. Beach, *J. Phys.: Condens. Matter* **9**, 3713 (1997).
- <sup>31</sup>A.V. Samoilov, G. Beach, C.C. Fu, N.-C. Yeh, and R.P. Vasquez, *Phys. Rev. B* **57**, 14 032 (1998).
- <sup>32</sup>R. Ganguly, I.K. Gopalakrishnan, and J.V. Yakhmi, *Physica B* **271**, 116 (1999).
- <sup>33</sup>K. Muta, Y. Kobayashi, and K. Asai, *J. Phys. Soc. Jpn.* **71**, 2784 (2002).
- <sup>34</sup>S.A. Baily, M.B. Salamon, Y. Kobayashi, and K. Asai, *Appl. Phys. Lett.* **80**, 3138 (2002).
- <sup>35</sup>S.A. Baily and M.B. Salamon, *J. Appl. Phys.* **93**, 8316 (2003).
- <sup>36</sup>In Ref. 34 a  $\text{La}_{0.85}\text{Ca}_{0.15}\text{CoO}_3$  single crystal was used, but unfortunately no details of the single crystal growth are given.
- <sup>37</sup>G. Maris, Y. Ren, V. Volotchaev, C. Zobel, T. Lorenz, and T.T.M. Palstra, *Phys. Rev. B* **67**, 224423 (2003).
- <sup>38</sup>S.B. Patil, D.K. Chakrabarty, M.V. Babu, and S.N. Shringi, *Phys. Status Solidi A* **65**, 65 (1981).
- <sup>39</sup>V.G. Bhide, D.S. Rajoria, C.N.R. Rao, G. Rama Rao, and V.G. Jadhao, *Phys. Rev. B* **12**, 2832 (1975).
- <sup>40</sup>P. Mandal and B. Ghosh, *Phys. Rev. B* **68**, 014422 (2003).
- <sup>41</sup>H.Y. Hwang, S-W. Cheong, P.G. Radaelli, M. Marezio, and B. Batlogg, *Phys. Rev. Lett.* **75**, 914 (1995).
- <sup>42</sup>B. Dabrowski, K. Rogacki, X. Xiong, P.W. Klamut, R. Dybziński, J. Shaffer, and J.D. Jorgensen, *Phys. Rev. B* **58**, 2716 (1998).
- <sup>43</sup>L.M. Rodríguez-Martínez and J.P. Attfield, *Phys. Rev. B* **54**, R15622 (1996).
- <sup>44</sup>R.D. Shannon, *Acta Crystallogr., Sect. A: Cryst. Phys., Diffr., Theor. Gen. Crystallogr.* **32**, 751 (1976).
- <sup>45</sup>We could also use the A-site ionic radii for 12-fold coordination as is done, e.g., in Ref. 42. This would cause quantitatively different parameters, but the main qualitative conclusions remain unchanged.
- <sup>46</sup>Since we have not grown a single crystal of  $\text{La}_{0.8}\text{Sr}_{0.2}\text{CoO}_3$  we used the corresponding  $T_c = 180$  K from Ref. 3.